SLAC-PUB-10666
August 2004

Effect of Dark Currents on the Accelerated Beam in an X-Band Linac*

V.A. Dolgashev, K.L.F. Bane, J. Wu, G.V. Stupakov, T. Raubenheimer

Stanford Linear Accelerator Center, Menlo Park, CA, 94025, USA

Abstract

X-band accelerating structures operate at surface gradients up to 120-180 MV/m. At these gradients, electron currents are emitted spontaneously from the structure walls (”dark currents”) and generate additional electromagnetic fields inside the structure. We estimate the effect of these fields on the accelerated beam in a linac using two methods: a particle-in-cell simulation code MAGIC and a particle tracking code. We use the Fowler-Nordheim dependence of the emitted current on surface electric field with field enhancement factor beta. In simulations we consider geometries of travelling wave structures that have actually been built for the Next Linear Collider project.

Paper presented at the Ninth European Particle Accelerator Conference (EPAC’2004), Lucerne, Switzerland, 5-9 Jul 2004

*Work supported by the U.S. Department of Energy contract DE-AC02-76SF00515.

EFFECT OF DARK CURRENTS ON THE ACCELERATED BEAM IN AN X-BAND LINAC *

V.A. Dolgashev, K.L.F. Bane, J. Wu, G.V. Stupakov, T. Raubenheimer,
SLAC, Menlo Park, CA, 94025, USA

INTRODUCTION

The metal surface of accelerating structures emits electron currents when operating at rf electric fields higher than 100 MV/m. These "dark currents" may have deleterious effects such as creating backgrounds for beam diagnostics, generating X-rays, loading rf power. They will also interact with the primary electron (or positron) bunch being accelerated in the structure, to kick the beam centroid (assuming that they are not axially symmetric) and they may dilute the beam emittance. For example authors of [1] suggest that such an interaction might have been a cause of beam jitter in SLAC Linear Collider (SLC).

In this report we study the effect of dark currents on the primary beam in 11.4 GHz travelling wave structures that were developed for the NLC [2]. The structures are disk-loaded waveguides with a near-constant on-axis gradient profile, designed to operate at 65 MV/m average gradient.

Experimental observations

During commissioning and operation of high gradient structures, dark current currents are routinely measured using current detectors, or by radiation detectors that monitor X-ray radiation induced by the currents. The exponential dependance of the measured currents on peak rf field is usually fitted to the rf Fowler-Nordheim curve [3].

$$I_F = 1.54 \times 10^{-6} \frac{\beta^2 A_e E^2}{\varphi} 10^{4.52\varphi^{-0.5}} e^{\left[-\frac{6.53\times 10^9 \varphi^{1.5}}{\beta E}\right]}. \quad (1)$$

Here I_F is current (in A), β the field enhancement factor, φ the work function of the metal (in eV), A_e the effective area (in m^2), and E the applied electric field (in V/m). After plotting the measured dependance of $\ln(I_F/E^2)$ *vs.* $1/E$, the slope gives β.

For X-band travelling wave structures tested at the NLC Test Accelerator (NLCTA) the β is typically found to be between 30 and 60, and for any given structure the measured β remains stable over time of operation. At the NLCTA the current is measured using a low-Q cavity located a few centimeters away from the output end of the structure, and the surface field is calculated from the known input power [4]. The typical downstream dark current during operation of an X-band travelling wave structure is about 1 mA (averaged over an rf pulse). The shape and amplitude of the pulse induced in the detector cavity is very reproducible from pulse to pulse. If a structure with filling time of 100 ns is excited by a short (50 ns) rf pulse, the output dark current pulse is about 150 ns, a result that indicates that there is uniform emission over the entire structure length. A few rf breakdowns do not significantly change the measured current. Also, if there are no rf breakdowns during the measurement, there is no obvious pulse width dependence of the dark current amplitude.

All the data above characterizes behavior of the dark current accumulated in a whole structure, but if we want to estimate the effect on the primary beam due to the current we need to know how many emitters there are in the structure, the current emitted by each one, and the location of the emitters. There is no experimental data on how many emitters there are and what their properties are for the NLC X-band structures. However, we conjecture that such parameters are similar to those found in high gradient rf guns and experiments where an image of emitters was obtained [5, 6]. These experiments show that current is emitted from localized sources with large source to source variation in intensity. A common conjecture for the origin of emitting spots on an rf gun cathode is that they occur at positions of earlier rf breakdowns. Usually the number of emitters is about 10 per few cm^2 of the cathode area [7].

MODEL

There are two steps in the simulation of the dark current induced kick on a primary beam: first, find the kick from a single emitter, and then, sum the effect of all emitters in a structure. To obtain the kick from a single emitter we have used two models: a 3D Particle-In-Cell (PIC) model of a few-cell structure and particle tracking for a whole, but simplified structure. To estimate the relation between the current emitted from a single emitter and the current registered by monitors outside the structure we use the particle tracking code [8]. We conjecture that secondary electrons do not contribute significantly to the kick.

Particle-In-Cell simulations

For 3D Particle-In-Cell simulations we use the commercially available code MAGIC3D [10]. We use as model of the accelerating structure a disk loaded waveguide with 120 degree phase advance per cell, cavity radius of 10.875 mm, period of 8.75 mm, iris radius 4.45 mm, and iris thickness 1.66 mm (the iris tip is rounded). A model developed for 3D self-consistent simulations of breakdown currents [11] was used for the dark current simulations. The model is built in cylindrical coordinates, with z = const being the (x, y) plane. The model consists of several regular cells (up to 10) and two coupler cells that match the impedance of a coaxial feed-waveguide to the impedance of the structure at frequency 11.424 GHz (with VSWR better then 1.2). Since the couplers are matched, the number of regular cells in the structure can be changed

* This work was supported by the U.S. Department of Energy contract DE-AC02-76SF00515.

without changing the VSWR to study the kick dependance on number of cells. An example geometry of such a structure that consists of one regular cell and two couplers is shown in Fig.1.

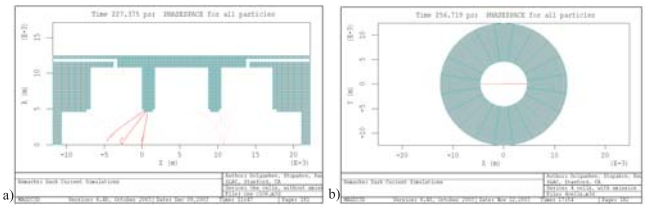

Figure 1: Snapshots of MAGIC3D screen with geometry of the travelling wave structure and electrons. a) (r, z) plane, b) (x, y) plane. Beam and rf energy move left to right in a); emission spot is at right in b), with $y = 0$. Emission spot is on upstream half of first iris.

To simulate dark current emission, the tip of an iris was divided into upstream and downstream parts. Then one half-tip sector was assigned to emit. The current emitted obeys the Fowler-Nordheim equation [12] with user-specified A, ϕ, and β. To set up the initial conditions a model of a structure (without emission) is first filled with 70 MW of rf power, and after one fill time all fields are dumped into a file. Then the simulation is restarted with one of the iris half-tips emitting for 10 – 20 rf cycles. During the run with emission, all components of electric and magnetic fields along trajectories of a primary beam are saved (with 2.4 ps time step).

Then the transverse kick caused by radial component of the the electric field and azimuthal component of the magnetic field is integrated, assuming the bunch moves with the speed of light.

Since PIC code does not separate the rf and dark current fields, we verified that the the kick normalized to average emitted current does not vary appreciably with changes in mesh, time step, and amplitude of emitted current.

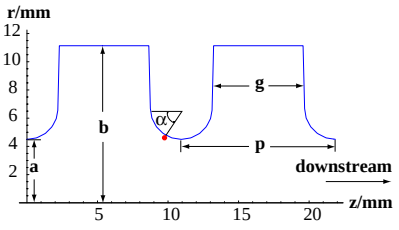

Figure 2: Two cells of the model geometry for particle tracking, showing the angle α (the emission point is given by the red dot).

Tracking

The PIC code has limitations that make it difficult to resolve questions related to position of the emitter on the iris tip or behavior of the dark current in 60 cm long structures. For example due to mesh size limitations of the PIC code, the smallest emitter size is ~ 1 mm, while emitters that are observed experimentally have sub-millimeter dimensions. Therefore, we use a particle tracking code to address these questions. Although particle tracking does not produce a self-consistent solution for rf and dark current fields, we found that qualitatively and quantitatively the results are very close to that of the PIC code.

The method we use for particle tracking and the results for outgoing dark currents are described in [8]. The method is based on a Mathematica code written by S. Setzer [9]. Here we provide details related to calculation of the dark current generated fields. In the simulations we use a geometry that corresponds to the average cell of an 11.424 GHz, 150 deg. phase advance travelling wave structure, with iris radius $a = 4.7$ mm, cavity radius $b = 11.1$ mm, gap $g = 6.9$ mm, and period $p = 10.9$ mm (see Fig. 2). First we calculate travelling wave fields for one period of the structure, then the Floquet condition is used to generate travelling wave electromagnetic fields in a whole 54-cell structure. For dark current calculations the amplitude of the field is normalized to produce an accelerating gradient of 65 MV/m in every cell.

Next we consider an iris emission point at angle α, defined with respect to the upstream horizontal (see Fig. 2). We allow charged macro-particles, initially at rest, to be pulled away from the walls by the rf fields. We let the time development of the charge of emitted particles follow the Fowler-Nordheim equation with $\beta = 30$.

We calculate trajectories of all macroparticles, and then electromagnetic fields induced by them on a primary beam moving along the z axis using Liénard-Wiechert potentials. Then we sum the kicks due to these fields to obtain the effect of a single emitter on the primary beam. Using this method we neglect fields of image charges induced by the macro-particle on the walls of the structure. We conjecture that this simplification does not change the kick significantly since most of dark-current – beam interaction takes place when the macro-particles "collide" with the beam.

RESULTS

We consider one emitter on the surface of an iris tip. This emitter could be a point at angle α (particle tracking) or a sector with $\sim$1 mm^2 (PIC code). We normalize the periodic emitted current to be 1 mA averaged over one rf cycle.

We find that most of dark current–beam interactions occur longitudinally in vicinity of the emitting iris. To demonstrate the localization of the kick we show in Fig. 3 the integrated $x-$kick as a function of z in a 10-cell structure for a beam on-crest (PIC code). The emitter is located at $z = 3.52$ cm, and this is where we observe a large kick. We also find that the kick (normalized to the average emitted current)is depends weakly on β.

Assuming the dark current particles are emitted with zero energy (*i.e.* zero initial emittance), the problem preserves up-down symmetry. The y component of the kick is zero if the primary beam y coordinate is 0, and it has

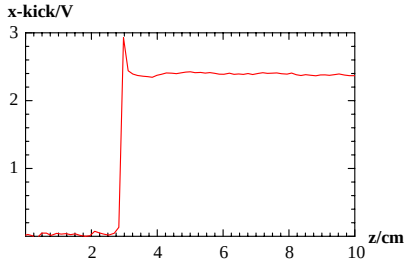

Figure 3: Accumulated kick *vs.* distance along the 10 cell structure for an on-crest electron bunch.

logarithmic singularity for $y \to 0$ or $y \to -0$. The x-kick weakly depends on shift of the beam trajectory from the structure axis.

The x and y–kick dependence on primary bunch rf phase, calculated using the PIC code are shown on Fig. 4. Coordinate $z_{off} = 0$ corresponds to an on-crest electron beam, $z_{off}/\lambda = \pm 0.5$ to on-crest positrons. Here λ is the rf wavelength. The x and y kick dependance on bunch phase for different α location of the emission spot, calculated using particle tracking is shown in Fig. 5. Here the y kick is integrated with the primary beam offset by 100 μm from axis. The amplitude of the kicks and the qualitative dependance on bunch phase look similar to the PIC results. We note differences between the two models: the size of emitters is different, and the geometries of the structures are different. We also note that in particle tracking, fields are integrated only for the one period of rf emission that has strongest interaction with the primary beam.

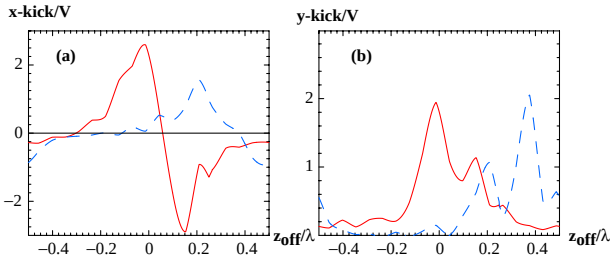

Figure 4: Amplitude of the transverse kick *vs.* bunch rf phase for different emitters calculated using the PIC code: upstream half-iris (solid) and downstream half iris (dashed). a) x-kick, beam on axis; b) y-kick for 250 μm offset in positive y-direction.

Dependance of x and y kicks on emitter position α for an on-crest electron bunch is shown on Fig. 6.

SUMMARY

We have calculated x and y transverse kicks induced on the primary beam by a single emitter of dark current in an X-band travelling wave accelerating structure. On-axis y kick is zero and x kick has a maximum amplitude of about 4 V per 1 mA of emitted current. From this we can roughly estimate the total kick for an on-axis beam. Assuming that

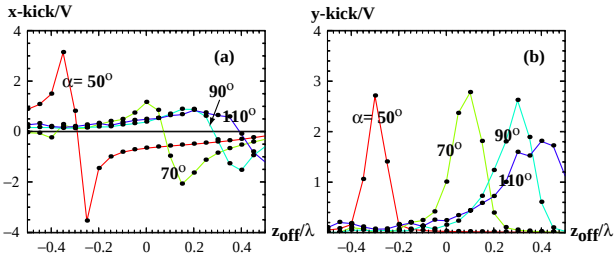

Figure 5: Amplitude of the transverse kick *vs.* bunch rf phase for different α location of emitters calculated using particle tracking. a) x-kick; b) y-kick for 100 μm offset in positive y-direction.

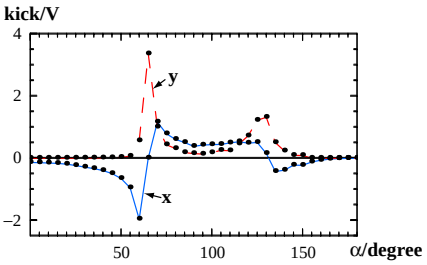

Figure 6: Amplitude of x and y transverse kick *vs.* position of emitter for on-crest electron bunch.

1 mA of outgoing current is 3% of total emitted current [8] and assuming one emitter on each iris (54 emitters in all), maximum kick is $4/0.03/\sqrt{54} = 18$ volts, a small number compared to the typical NLC-beam wake field deflection. We note that the main reason for such a small kick is the small emitted charge: for 1 mA of average emitted current, charge integrated over in one rf cycle is 0.088 pC. The interaction of the beam with larger currents generated in the structures by rf breakdown is a subject for further study.

REFERENCES

[1] C. Adolphsen and T. Slaton, SLAC-PUB-6905, Proceedings of the PAC95, 1995.

[2] C. Adolphsen, ROPC006, Proceedings of the PAC03, 2003, pp. 668 - 672.

[3] J. Wang, Ph.D. thesis, SLAC Report 339, 1989.

[4] C. Adolphsen and S. Döebert of SLAC, private communication.

[5] P. Gruber, *et al.*, TPAB091, Proceedings of the PAC03, 2003, pp. 1413 - 1415.

[6] X. Wang, Ph.D. thesis, UCLA, 1992.

[7] D. Palmer of SLAC, private communication.

[8] K.L.F. Bane *et al*, paper TUPKF059, this conference.

[9] S. Setzer, *et al*, Proc. PAC03, 3566 (2003).

[10] http://www.mrcwdc.com/Magic/

[11] V.A.Dolgashev *et al.*, SLAC-PUB-8866, Proceedings of the PAC01, 2001, pp. 3807 - 3809.

[12] R. Fowler, L. Nordheim, *Proc. Roy. Soc* **A119**, 173 (1928).